19th International Conference on
Adaptive Structures and Technologies
October 6-9, 2008
Ascona, Switzerland

Distributed Damping of Large Structures

Andrea Bergamini[1]*, Rouven Christen[2], Masoud Motavalli[2], and Paolo Ermanni[3]
[1] Empa, Laboratory for Mechanics for Modelling and Simulation, Switzerland
Überlandstrasse 129, CH-8600 Dübendorf, T.+41 44 823 4424, F. +41 44 823 4252, andrea.bergamini@empa.ch
[2] Empa, Laboratory for Structural Engineering, Switzerland
[3] ETH Zurich, Institute of Mechanical Systems (IMES), Centre of Structure Technologies

ABSTRACT

Adaptive systems are typically viewed as a suitable combination of a base structure (plant) that is enhanced with actuators that act on it based on the input from a controller that compares the actual trajectory of the system with the desired one. While very intensive research is carried out on the latter two elements (actuators and controllers), the effect of variable mechanical impedance of the former (plant) on the global behavior of an adaptive system is generally less exhaustively investigated. The present work deals with the modification of the mechanical properties of simple beams. The application of an electrostatic field between two adjacent layers of a multi-layer beam is expected to be an effective method to modulate the amount of shear stress that can be transferred at the interfaces. This modification of the shear stress transfer within a multi-layer structure and consequently of its stiffness was originally thought as an elegant approach to the suppression of resonant vibrations. While the viability of this approach could be demonstrated in certain cases, the limited shear strength of the electrostatically coupled interfaces currently represents a constraint to its usability for stiffness switching purposes. When the shear strength of the interfaces is exceeded, slipping occurs at the interfaces. A closer look at this situation (that was initially considered as undesirable) has lead to the investigation of the damping properties of electrostatically coupled multi-layer beams. These structures have shown good damping behaviour. First measurements show that a friction damping component is superimposed on the viscous damping of the base (not activated) structure. A more detailed investigation and the consideration of possible applications are planned for the near future.

Keywords: Variable Stiffness, variable damping, distributed damping, shear stress transfer layer.

1. INTRODUCTION

An adaptive structure can be represented as system consisting of a host structure on which actuators act in order to modify its state or trajectory according to a prescribed pattern. In order to do so, sensors are needed to determine the actual state of the structure and a controller is needed to provide the necessary 'intelligence' to appropriately drive the actuators. Under these assumptions, the mechanical properties of the host structure are considered invariant (figure 1a)).

The development of structures that have the ability to change their mechanical properties in a controlled way, in response to an external stimulus holds the promise to expand the freedom in the design of adaptive structures, as outlined in figure 1b). For actuated structures, the additional freedom resides in the ability to change the mechanical impedance of the structure so as to adapt it to the power output of the actuator that acts on it. As a hypothetical example to illustrate the use of variable

impedance structures, one can imagine a morphing load bearing structure that has a high stiffness under most operational conditions and whose stiffness is reduced in concomitance with the morphing process. This use of variable stiffness, discussed in [1] allows for a reduction of the power needed for the actuation and thus for a reduction of the size of the actuators [2-4].

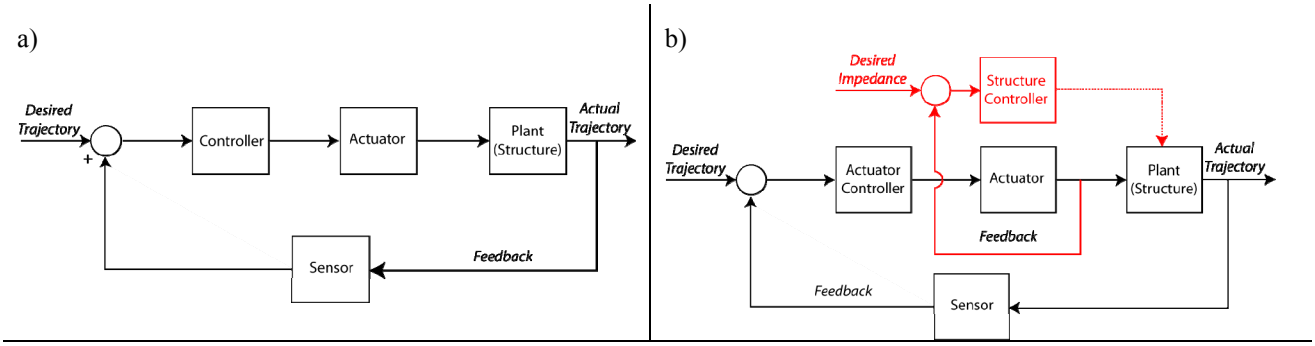

Figure 1 Left: schematic representation of a typical adaptive structure, consisting of a plant (host structure), one or more actuators, sensor(s) to determine the actual trajectory of the system and a controller to determine the adequate energy input from the actuator. Right: representation of an augmented adaptive structure, in which not only the energy input from the actuator but also the mechanical impedance of the structure can be controlled.

The present article gives an overview of the investigation of the mechanical properties of passive structures with variable stiffness and damping. The use of such structures is expected to allow for the suppression of high amplitude vibrations either as a consequence of the modification of their eigenfrequency or of increased damping. [5-10]

2. ELECTROSTATIC MODIFICATION OF THE BENDING STIFFNESS AND DAMPING PROPERTIES OF MULTI-LAYER STRUCTURES

2-1. Modification of the bending stiffness

The difference between the bending stiffness of a laminated multi-layer structure and one where the layers are loose is given essentially in the fact that in the laminated structure, shear stress is distributed on the entire cross section of the structure. In the loose bundle of unlaminated layers, the shear boundaries of the shear stress distribution are given by the surfaces of the individual bundles, as shown in figure 2. The shear stress distributions for the unlaminated beam (left) and for the laminated beam (right) are calculated for the case of cantilever beams subjected to a distributed transversal load. In laminated structures, the creation of covalent bonds between the layers leads to the cancellation of the boundaries within the structure and thus to the modification of the mechanical properties.

Any method that allows for the modulation of the shear stress transfer within a multi-layer structure can thus lead to the modification of its bending stiffness. For practical applications, a number of additional conditions must be satisfied by such a stiffness switching method:

- The amount of energy needed for changing the stiffness should be as small as possible
- The time needed for the switching should be short
- While activated the interfaces should ideally transfer large amounts of shear stress, so as to withstand large external loads

Under ideal conditions, the modification of the stiffness will not affect the damping properties of the system, as long as no inelastic processes take place at the interfaces.

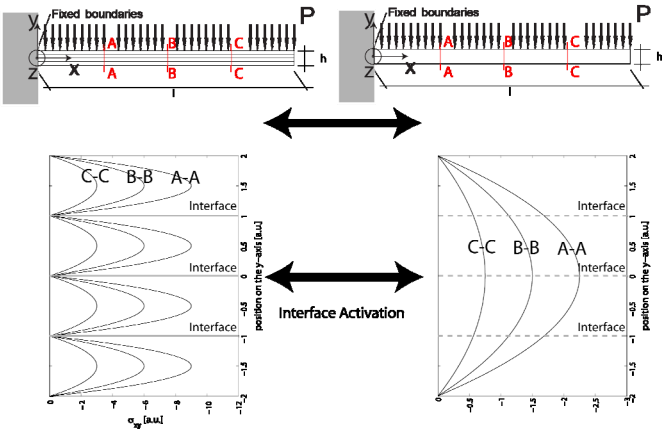

Figure 2: Effect of the cancellation of interfaces in a 4 layer beam on the shear stress distribution in three different cross sections. The change in shear stress distribution is at the origin of an increase in stiffness of the system

The method for the modification of the shear stress transfer properties of interfaces investigated in the past few years is based on the use of attraction forces that can be generated by applying an electrostatic field at the interfaces of a multi-layer system, as shown in figure 3. The interfacial stress is a function of the electrostatic field, as given by (1):

$$\sigma_{yy}^{\text{int}} = \frac{\varepsilon\varepsilon_0 U_i^2}{2\delta^2} \tag{1}$$

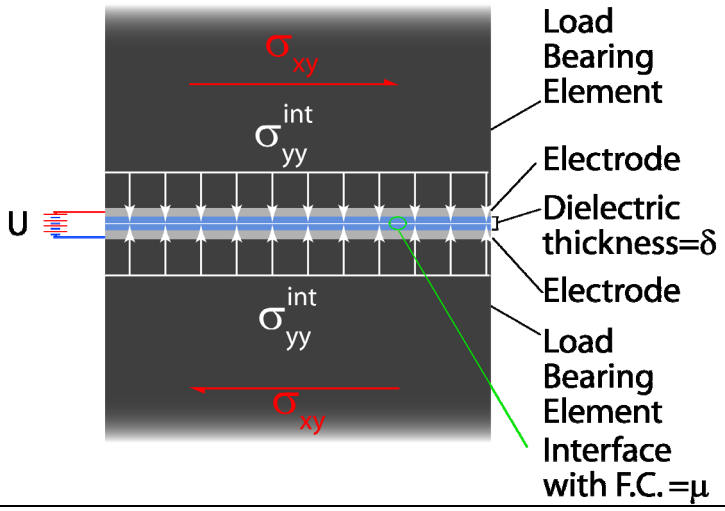

Figure 3: Modification of the ability to transfer shear stress by means of electrostatic attraction forces.

Under normal conditions, the contact at the interfaces implies the appearance of friction if a shearing force is applied across them. As long as the applied shearing force, divided by the apparent area of contact, does not exceed the value given by (2), no relative displacement between the contact surfaces will take place. Hence the shear stress σ_{xy} is transferred across the interface, as if they did not exist.

$$\sigma_{xy}^{\max} = \mu\sigma_{yy}^{\text{int}} \tag{2}$$

The experimental verification of this hypothesis is a quite demanding task, as the behavior of

the system is strongly influenced by the boundary conditions of the experiment and by the planarity of the contact surfaces. These are assumed to be ideally planar when considering the amount of shear stress that needs to be transferred at the interfaces. In reality, experiments and observations have shown, that this is not the case. Even materials that, for most purposes, are considered as planar present considerable curvatures. Figure 4a shows the experimental set up of a two-layer cantilever beam consisting of two plates cut from a silicon wafer. The two 400µm plates were electrically insulated by means of a 400nm thermal oxide layer. By applying a potential between the two layers, the shear stress transfer at the contact surface could be increased. Under ideal circumstances, the stiffness was expected to increase by a factor of four, hence the first bending eigenfrequency was expected to double. The frequency response (figure 4b) obtained experimentally, shows that while no substantial broadening of the resonance peaks is observed, the frequency of the first bending mode is only shifted to a 40% higher value for the highest interlaminar voltage level U=200V. At a lower voltage level, a more modest frequency shift is observed, while no obvious peak broadening is seen. While no in-depth investigation of the reasons for this behavior has been carried out, the interpretation so far is that due to the different curvature of the two plates only partial contact between them can be achieved.

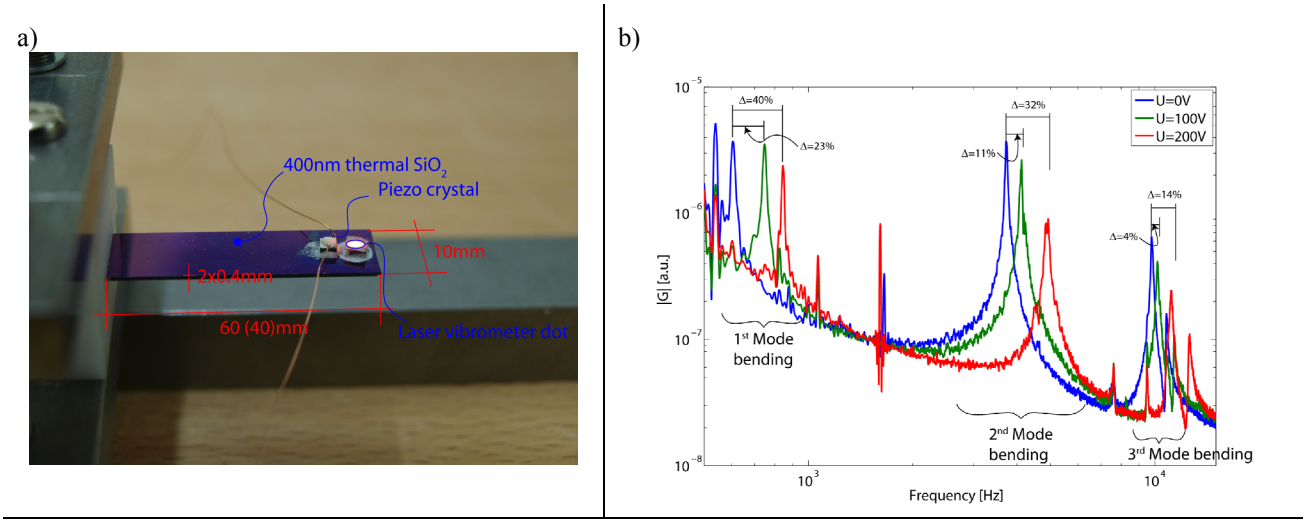

Figure 4: Left: Experimental set up consisting of two stacked silicon wafer cantilevers excited by a piezo-crystal. Right: Frequency response measured at excitations between 500 Hz and 20000 Hz at three different interlaminar voltage levels U_i

Previous work [11] has shown that the ratio between curvature of the elements of a multi-layer structure to bending stiffness of the elements correlates to the normal stress needed to obtain contact between the surfaces. Furthermore, the presence of a gap between the layers increases the distance between the electrodes and thus has an unfavorable effect on the electrostatic stress generated by the field.

2-2. Modification of the damping properties

The considerations of the previous section show that there are some limitations to the implementation of electrostatic stiffness modification. In most cases, the lack of ideal interface geometries in presence of considerable transversal loads lead to a situation where the shear stress at the interfaces exceeds the ability of the system to transfer it completely by means of friction. This situation is shown in the shear stress distribution plot shown in the bottom right part of figure 5. The solid lines in the plot show the parabolic shear stress distribution calculated analytically for a solid beam of height *h*, as shown the figure. The dotted lines show the shear stress distribution calculated

numerically for a beam consisting of four layers, each with thickness h/4, coupled at the interfaces by a normal stress σ_{yy}= 3 MPa, considering the friction coefficient μ=0.2. Both shear stress distributions are calculated under the assumption of a distributed transversal load acting on a cantilever beam, as shown in the sketch at the top of the figure. The maximum shear stress that can be transferred at the interface is 600 kPa, as can be calculated with (2). The plots shown in figure 5 show that, based on numerical calculations, the shear stress level in correspondence with the interfaces is indeed limited to approximately 600 kPa. The deviation between the parabolic shear stress distribution expected in an slender solid beam and the distribution calculated for a multi-layer beam confirms the limitation imposed by the interface and indicates the appearance of a non-linear behavior.

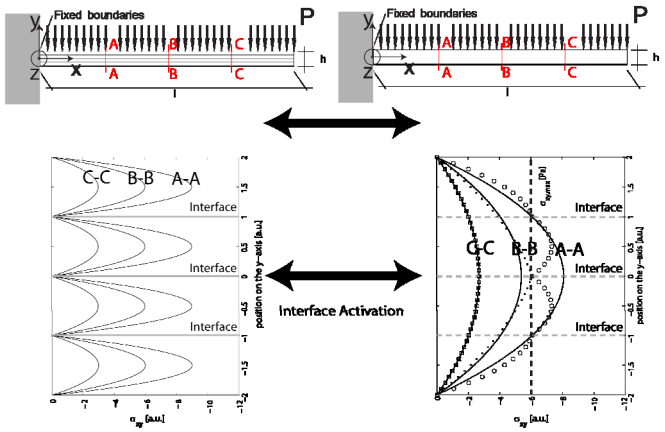

Figure 5: Effect of the cancellation of interfaces in a 4 layer beam on the shear stress distribution in three different cross sections, when the shear stress at one interface exceeds the interface's ability to transfer it in full.

Figure 6 shows four force-displacement diagrams calculated for different levels of interfacial stress for linear loads up to 1500 N/m. The results of the calculations show that the increasing interfacial stress levels lead to an increase of the load at which the behavior of the beam begins to deviate from linear elastic. This is made plausible by the fact that the limit imposed by the interfaces' ability to transfer stress is increased.

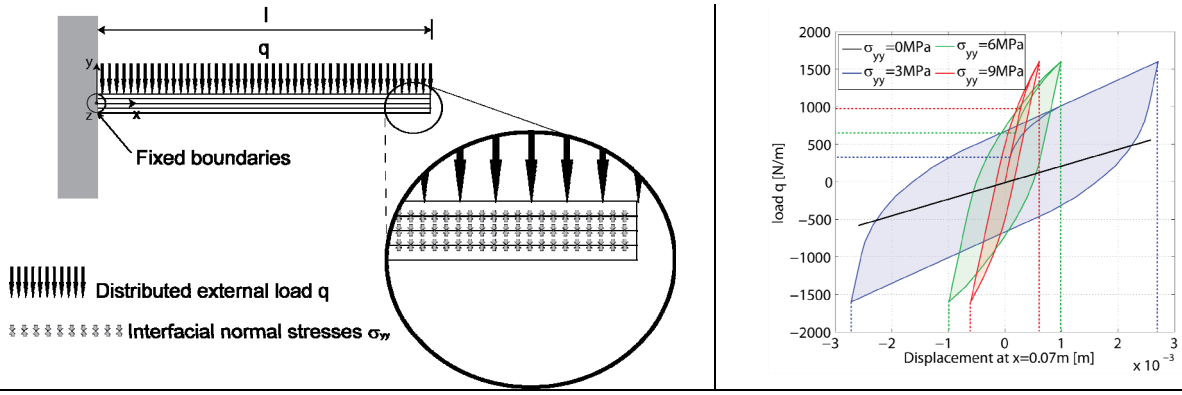

Figure 6: Left: Sketch of the model used for the numerical calculation of the hysteretic behavior of a homogeneous 4 layer beam. Right: Hysteretic behavior of the system as a function of the interlaminar normal stress.

The hysteretic behavior of the system shown in figure 6 suggests that when cyclically loaded beyond the shear strength of the interfaces, electrostatically coupled beams can dissipate variable amounts of mechanical energy, depending on the area included within the hysteresis. The experimental work described in the following sections was aimed at investigating the effect of electrostatic coupling on the damping behavior of the described structures.

3. EXPERIMENTAL WORK

In the set up used for the experiments, the bond between additional stiffening elements (CFRP plates, CarboDur M614, Sika, CH) and the core of the sandwich beam (GFRP I-beam, Fiberline Composites, DK) is given by electrostatic forces generated by an electrical field built up across a 12 μm thick polyethyleneterephtalate (PET, $\varepsilon_r \approx 1$, Amcor Flexibles, Burgdorf, CH) film that was coated with a thin aluminum film on one side (coating thickness unknown). The PET film was applied to the flanges of the GFRP beam using epoxide resin (Araldit Standard, Vantico AG, Basel, CH). The CFRP plates served at the same time as second pair of electrodes and stiffening member. This setup was chosen in order to optimize the electrostatic forces that could be obtained per unit voltage. The multi-layer beam was fixed on one end and excited at the free end by means of the electromagnetic fields generated by a coil, acting on a 40 mm x 40 mm x 20 mm FeNdB permanent magnet that was attached to the end of the beam, 2240 mm from its fixation point. The brackets visible in the left hand side of Figure 7 were only used to keep the loose CFRP plates in place when the electrostatic field was turned off, ideally without exerting any normal forces. Two additional masses (1050 g each) were placed 2090 mm (position of the center of gravity) from the fixed end of the beam to help separate the first bending and torsion modes of the beam. The current necessary to induce the exciting alternate magnetic field, was generated by a bipolar operational power amplifier (BOP 20-20 M, Kepco, USA) driven in its current controlled mode by an arbitrary signal generator (33120 A, Agilent, USA). The transversal accelerations at the end of the composite beam were measured by means of two accelerometers (PCB Piezotronic, Mod. 3701 G3 FA3 G, with a sensitivity of 1 V/g) positioned at the left and the right edges at the free end of the beam (sensor 1 and sensor 2, respectively). The current circulating through the coil was measured using a shunt resistor connected in series with the coil. The shunt had a resistivity of 0.01 Ω (60 mV/6 A). The acceleration and the current circulating through the coil were measured with a sampling frequency of 512 Hz using an OROS 38 data acquisition system. The components of the sandwich beam were connected to a high voltage power supply (PS 350, Stanford Research Systems, USA), so that the necessary electrical potential U_i could be applied between faces and core.

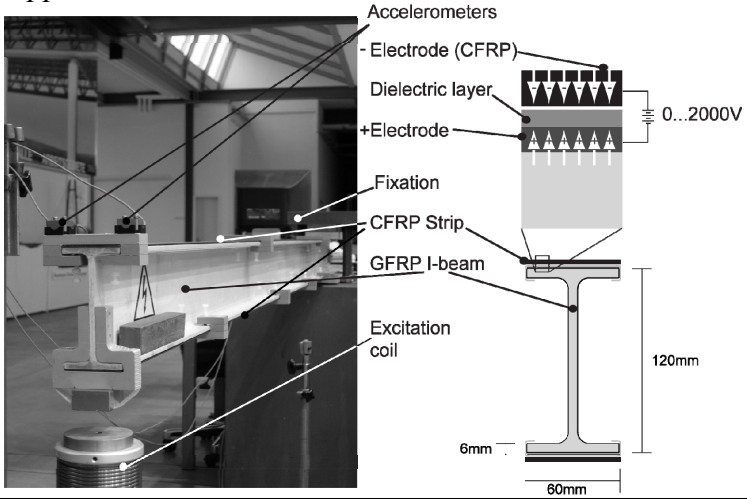

Figure 7: Test Set-up used to investigate the effect of electrostatic coupling on the damping behavior of multi-layer beams. In this set-up the layers are not homogeneous: The two outer layers have a high stiffness (CFRP Strips) while the core has a lower tensile and shear stiffness (GFRP I-beam)

In order to investigate the damping properties of the system, the beam was excited in its eigenfrequency with varying current amplitudes. The excitation current was then turned off and the decaying vibration was recorded. From these measurements the amplitude decay of the vibration was

calculated as the absolute value of the Hilbert transform of the measured signal. As shown in figure 8, the amplitude decay curves measured in the described experiments deviate from the ideal exponential decay that would correspond to pure material damping. This is explained by the hysteretic behavior discussed in the previous section that is superimposed to the materials damping of the structure. Strictly speaking it is thus incorrect to calculate a logarithmic decrement based on the measured decay curves. Nevertheless, for a well defined portion of the decay curves, the calculation of an equivalent logarithmic decrement may represent a valuable, if not completely accurate way to obtain a comparison of the damping obtained by means of friction with other damping methods.

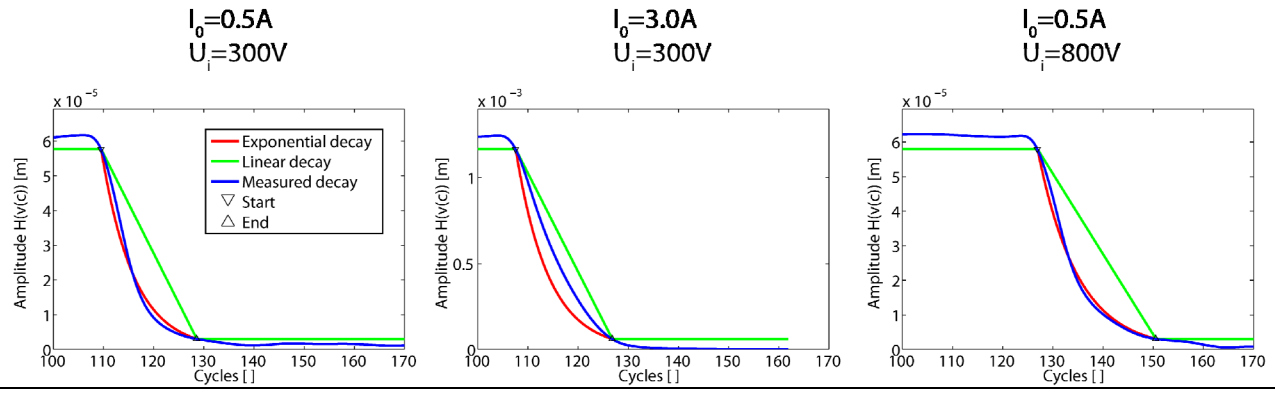

Figure 8 Measured amplitude decay curves (blue) for different values of the excitation current amplitude I_0 and interlaminar voltage U_i. The red curves represent a purely exponential decay as would be expected for material damping, the green curves represent a linear decay, as would be expected for friction damping. The exponential and linear curves are calculated for amplitudes between 95% and 5% of the initial amplitude of the vibration.

4. RESULTS AND DISCUSSION

The measurements confirm the trend according to which at all excitation amplitudes an increase in electrostatic potential U_i induces a shift of the first bending eigenfrequency to higher values (as shown in the left hand plot) reaching the highest value for the highest voltage.

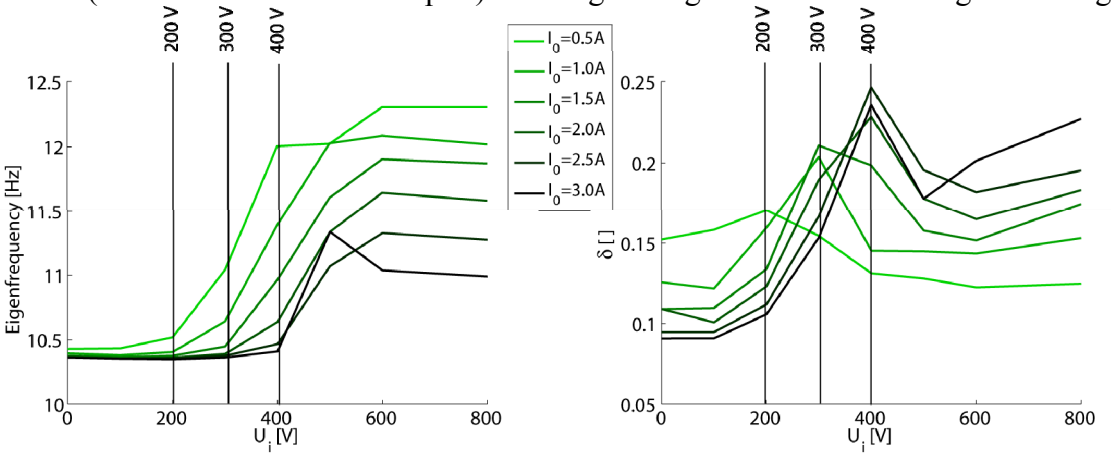

Figure 9 Left: Measured 1st bending eigenfrequency as a function of the excitation amplitude I_0 and the interlaminar stress U_i. Right: Estimated damping ratio as a function of the excitation amplitude I_0 and the interlaminar stress U_i, calculated as described above.

The plot on the right hand side of figure 9 shows the development of the equivalent logarithmic decrement δ as a function of interlaminar voltage for different excitation amplitudes. This plot shows clearly that the damping properties reach a maximum level at intermediate voltage, while

they are lower when no voltage or a high voltage level is applied.

The voltage dependent hysteretic behavior shown in figure 6 is a plausible explanation for the effects shown in figure 9: When no voltage is applied, the interaction between the layers of the system can be expected no or negligible interaction. Ideally, no stiffening effect from the interaction between layers is observed, independently of the amplitude of the excitation. At the other end when high voltage is applied, for sufficiently weak excitation, the layers are expected to behave as if they were laminated, thus leading to an increase in stiffness without an increase in damping, as shown by the bright green curves in figure 6 (I_0=0.5A). According to the behavior shown in figure 6, the area within the hysteresis varies as a function of the interlaminar stress. For intermediate combinations of excitation amplitude and interlaminar voltage, a combination of increase in stiffness and damping can be observed (figure 9), with the damping reaching its maximum at voltage levels between the ones associated with minimum and maximum stiffness.

For vibration mitigation purposes, a modification of the bending stiffness (and consequently of the eigenfrequencies of the bending modes) is expected to make a contribution to the reduction of the amplitude of resonant vibrations. Calculations performed on a numerical model of Empa's pedestrian cable stayed bridge (figure 10, left) show however that for a fairly highly constrained structure, such as this, the increase in stiffness obtained by applying unidirectional carbon fiber strips does not lead to a significant modification of the first bending eigenfrequency.. In the case considered in figure 10, the lamination of additional elements is expected to lead to an increase in stiffness of the order of 1.5 times.

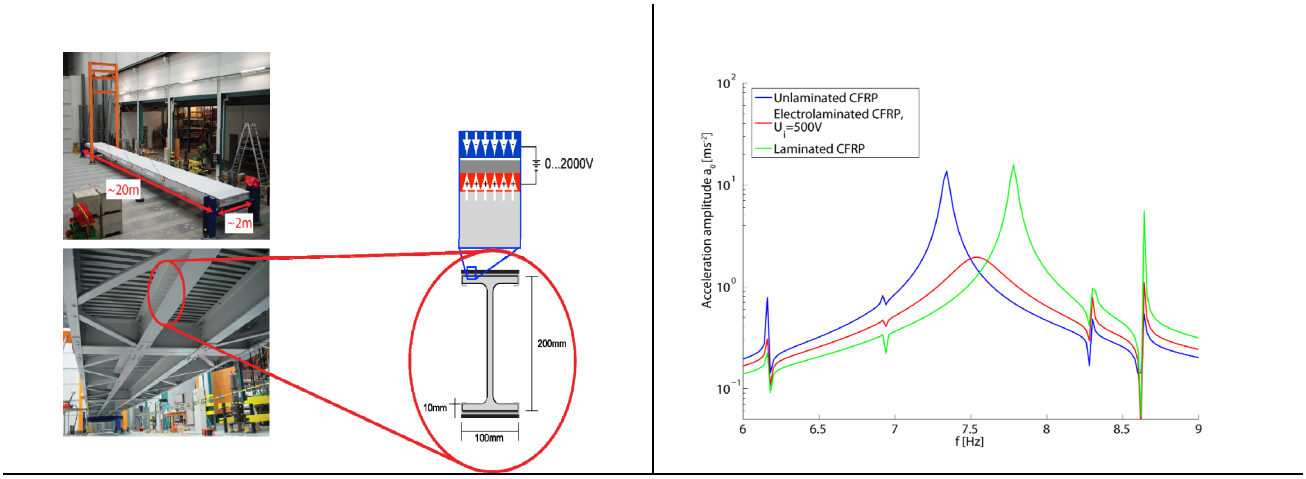

Figure 10 Left: Envisioned integration of electrostatically coupled stiffening elements. Right: Extraplolated dynamic response of Empa's pedestrian Bridge

Calculations performed based on a numerical model of the bridge, show that the frequency shift obtained by the stiffening of the deck is actually quite modest (from 7.3 Hz to 7.8 Hz), due to the complexity of the structures. The effectiveness of such a measure in the way of avoiding resonance phenomena is not guaranteed if the source of excitation does not present a narrow band energy spectrum. The predicted behavior for electrostatically coupled stiffening elements, based on measurements performed on individual beams as described in the previous section, shows that the damping contribution made by the hysteretic characteristic has a positive effect on the reduction of the vibration amplitude of the structure over the whole considered spectrum.

5. CONCLUSIONS

The electrostatic coupling of multi-layer structures has been shown to be essentially equivalent to the cancellation of the interfaces at low loads, where the shear stress at the interfaces

does not exceed their ability to transfer it. At higher load levels, the presence of interfaces subjected to a normal stress, as the shear stress cannot be transferred in full, slipping at the interfaces starts occurring. This situation is at the origin of the hysteretic character of the force-displacement behavior of the system that causes energy dissipation to take place.

Thus, electrostatically coupled multi-layer structures display two interesting properties: the ability to modify their bending stiffness and an increased the damping ratio of the system, at high load levels. Both properties have a significant use for the damping of structural vibrations.

The experiments performed on a fairly large CFRP-GFRP-CFRP sandwich beam presented in this contribution give and show the effect the electrolamination of stiffening elements onto a rigid structure on its damping behavior. The calculated envelopes of the decay of the free vibration of the structure show that the hysteretic effect is superimposed on the material damping of the beam. In order to obtain a rough comparison of the vibration damping performance of electrostatically coupled beams, an equivalent logarithmic decrement of the system was calculated on set portion of the decay curve between 95% and 5% of the initial vibration amplitude. The damping shows a maximum value for the interlaminar voltage levels that correspond to the transition between the low stiffness to the high stiffness level. This can be explained in terms of the area enclosed by the hysteretic load displacement diagram of the system.

The system properties determined in the experiment are used to describe the application of electrostatic damping to the GFRP deck of Empa's pedestrian bridge. Based on the properties of the investigated beam, the properties of the bridge deck model were calculated for three conditions of the target system: the unstiffened bridge deck, the bridge deck stiffened by laminating CFRP bands to it and finally the bridge deck with electrolaminated CFRP bands at conditions that yield the highest damping factor. Due to the fairly high level of constraint of the deck, the frequency shift obtained by laminating the CFRP bands is very limited. Depending on the band width of the exciting spectrum, the predicted frequency shift of approximately 0.5 Hz is likely not to be sufficient to suppress a high amplitude resonant vibration by disrupting the resonance situation. The ability of the system to realize quite high levels of damping represents a more vi-able approach to the suppression of structural vibrations.

REFERENCES

1. Gandhi, F., and Kang, S.-G., "Beams with Controllable Flexural Stiffness," Smart Materials and Structures, Vol. 16, No. 4, pp. 1179-1184, Aug. 2007
2. Marden J.H., "Scaling of maximum net force output by motors used for locomotion", The Journal of Experimental Biology 208, 1653-1664, 2005
3. Henry, C. P.; McKnight, G. P.; Enke, A.; Bortolin, R.; Joshi, S.,. "3D FEA simulation of segmented reinforcement variable stiffness composites," Proc. SPIE, 6929:1-12, 2008
4. Gordon B. O. and Clark. W. W. "Morphing structures by way of stiffness variations". 49th AIAA/ASME/ASCE/AHS/ASC Structures, Structural Dynamics and Materials Conference, vol. 1, 183–191, 2007
5. Kornbluh, R. D.. Prahlad H, Pelrine R., Stanford S.,. Rosenthal M. A, and von Guggenberg. P. A. "Rubber to rigid, clamped to undamped: toward composite materials with wide-range controllable stiffness and damping". Proc. SPIE 5388, no.1, 372–386, 2004.
6. Brennan M.J. Actuators for active vibration control-tunable resonant devices. In 4th Euro Conf on Smart Structures and Materials,, pages 41–48, 1998
7. Onoda J, Endo T, Tamaoki H and Watanabe N, "Vibration suppression by variable-stiffness members" AIAA J., 29, 977-983, 1991
8. Høgsberg J. and. Krenk. S "Adaptive tuning of elasto-plastic damper" International Journal of Non-Linear Mechanics, 42(7):928-940, September 2007.
9. Goodman L.E. and Klumpp J.H. (1956), Analysis of slip damping with reference to turbine-blade

vibration. Journal of applied Mechanics 23, 421-429
10. Tabata O., Konishi K. et al.. Micro fabricated tunable bending stiffness devices. Sensors and Actuators A, 89:119–123, 2001.
11. Bergamini A., ETH Dissertation 'Electrostatic Modification of the Bending Stiffness of adaptive Structures, Zurich, under evaluation